Optical and near-UV spectroscopic properties of low-redshift jetted quasars in the main sequence context

Shimeles Terefe

Ascensión Del Olmo (IAA-CSIC, Spain), Paola Marziani (OAPd-INAF, Italy), Mirjana Pović (SSGI & IAA-CSIC) and collaborators

2026 African Astronomical Society Conference, 22 – 27, March, 2026, Botswana/Kasane

Introduction, Quasars

- First discovered in 1963 (Schmidt, 1963, Kellermann, 2013).
- They are the most distant and luminous objects in the universe with $L \geq 10^{48}$ ergs s^{-1} (Bloom et al. 2009).
- They show unusual optical emission spectra unlike those of stars (Kellermann, 2013).
- Considering their radio emission, typically classified into (Begelman et al. 1984):
  - Radio loud (RL)
  - Radio quiet (RQ)
- Considering physical difference, can be classified as (Padovani, 2017):
  - Jetted
  - Non-jetted

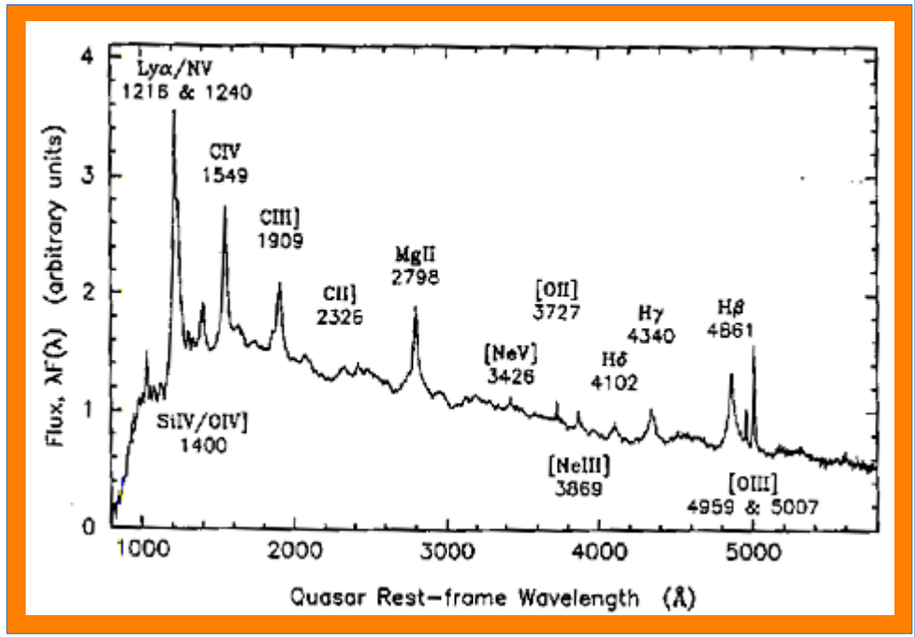

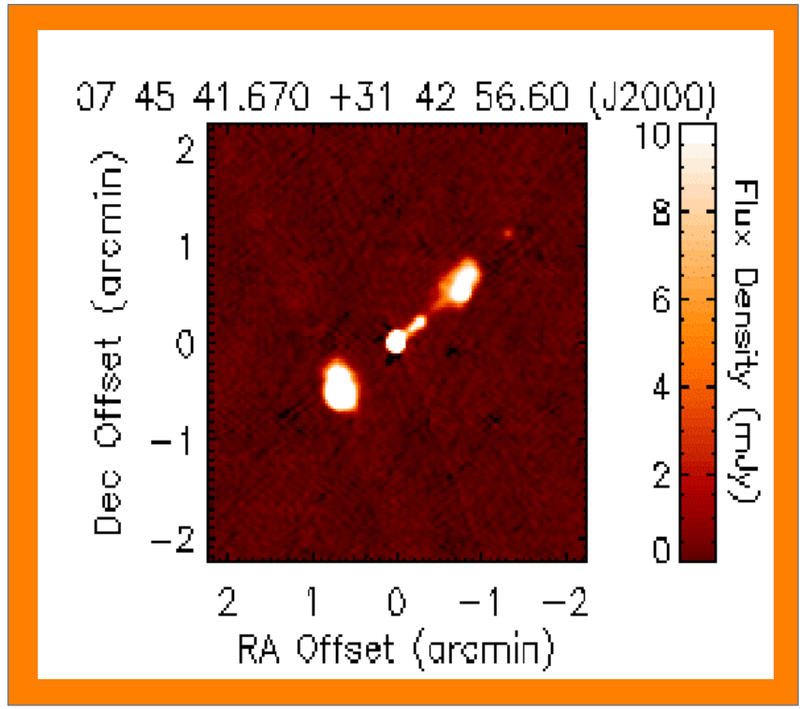

Fig. Composite spectrum of a quasar (top, Francis et al. 1991) and FIRST cutout image of the quasar 4C 31.3 (bottom).

Data: New and archival

- **New optical and near-UV spectra: CAHA 3.5m telescope (Spectra of MgII, Hβ, Hα lines)**

- **Astronomical archival data**
  - **Radio: NVSS and FIRST (Radio flux at 1.4 GHz)**

  - **UV: HST (For CIV and CIII])**

  - **Optical: SDSS**

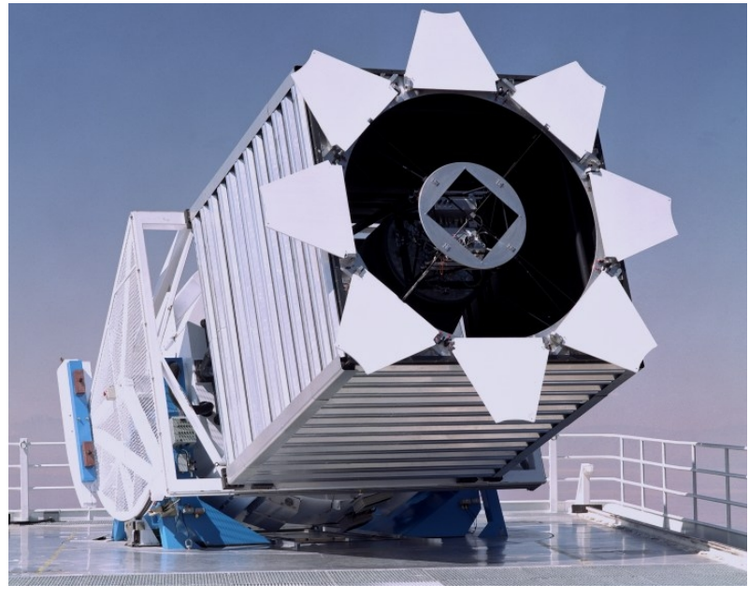

Data

- **New optical and near-UV spectra:**
  - **12 RL quasars with 0.35 < z < 1,**
  - **Radio loudness, > 1000,**
  - **logP_v > 33 [ergs s^{-1} Hz^{-1}],**
  - ***LogL_{bol} ~ 44.9 – 46.7* [ergs s^{-1}]**

$$R_k = \frac{f_{1.4GHz}}{f_g}$$

- **Comparison samples:**
  - **Optical: *Marziani et al. 2003* and *Zamfir et al. 2010.***
  - **Near-UV: Wang et al. 2009, Marziani et al. 2013 and Calderone et al. 2017.**

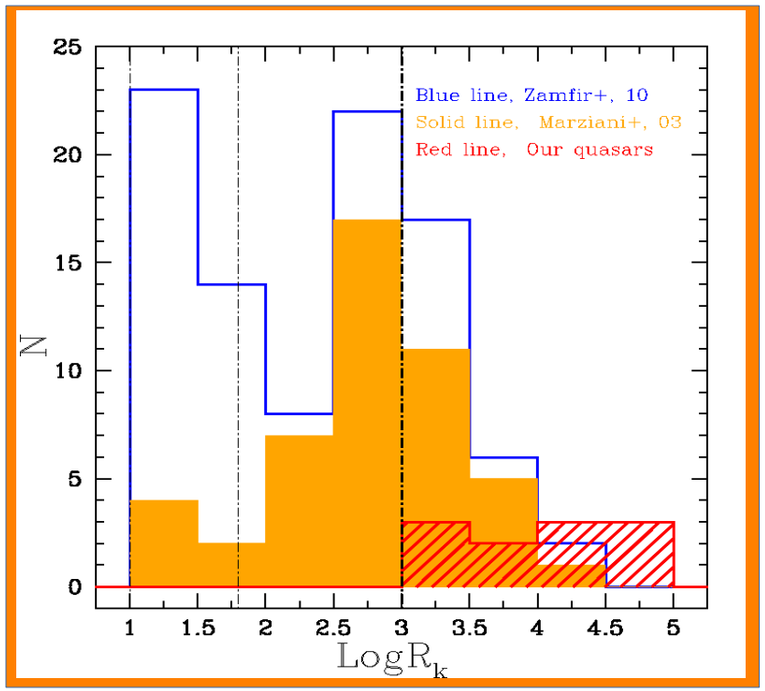

Fig. : Distribution of R_k for Pop. B RLs.

Table 1: Summary of main comparison samples and this work sample

Information	Marziani+03	Zamfir+10	Marziani+13[a]	This work[b]
Redshift range	z < 0.8	z < 0.7	0.4 < z < 0.75	0.35 < z < 1
No. of sources	168	469	8[a]	12
Parameters	c($\frac{1}{2}$), c($\frac{1}{4}$), R_K FWHM,AI	c($\frac{1}{4}$), R_K, AI FWHM,$R_{FeII,opt}$	c($\frac{1}{2}$), c($\frac{1}{4}$) FWHM,AI	c($\frac{1}{2}$), c($\frac{1}{4}$), R_K FWHM, AI $R_{FeII,opt}$,$R_{FeII,UV}$[b]
Lines used	Hβ	Hβ	Hβ and MgII	Hβ and MgII
Log L_{bol}[ergs s^{-1}]	43.7–47.8	43.0–47.0	45.7–46.9	45.15–46.57
No. Pop. B RLs:				
logR_K>1.8	42	61	–	12
logR_K>3	17	25	–	12
logR_K>4	1	2	–	7

Method

- **Emission lines analyzed by doing three complementary approaches:**

1. **Multi-component non-linear fitting using the *IRAF* task "*specfit*" for the 12 jetted quasars**
2. **Full broad profile analysis**

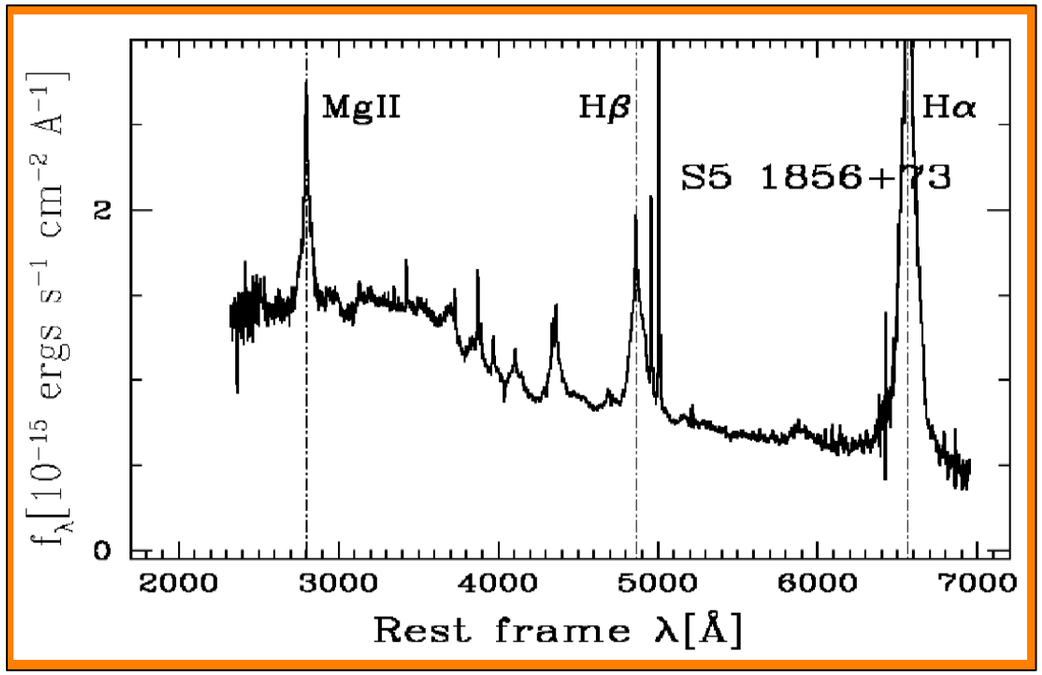

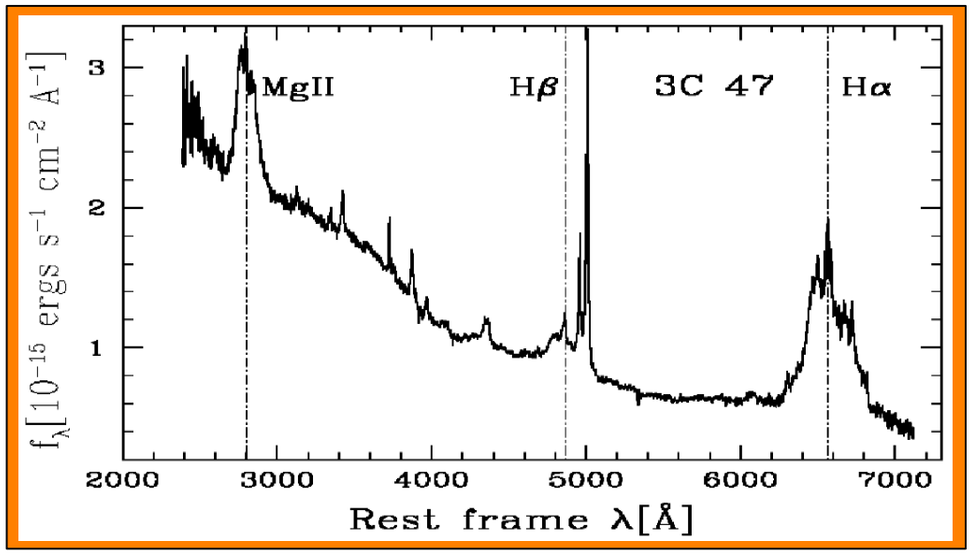

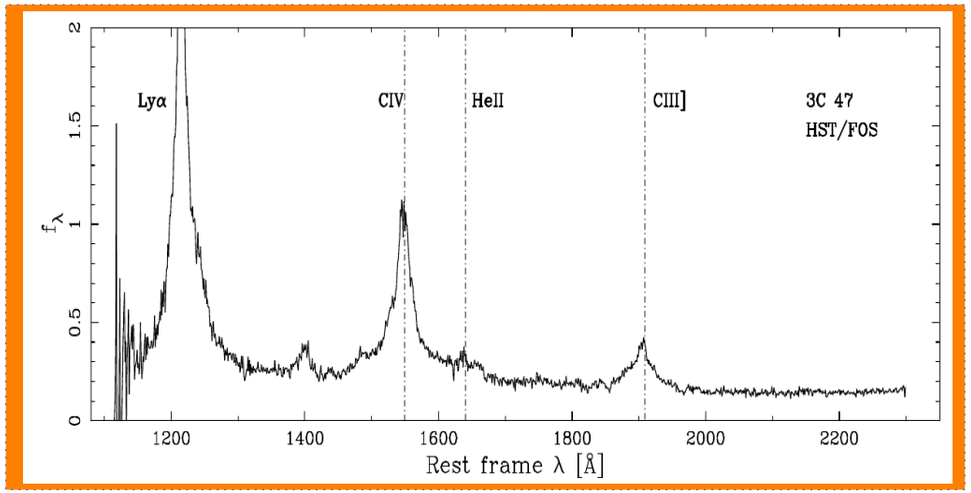

Fig. Rest frame spectra of the quasar S5 1856+73 (left) and 3C 47 with the prominent emission lines in the near-UV, optical and UV (right bottom) regions .

Method : 1. Spectral fitting Hβ

❖ **Simultaneously fitting all the following components:**

Continuum

$$F_\lambda^{cont} = F_\lambda^{PL} + F_\lambda^{FeII}$$

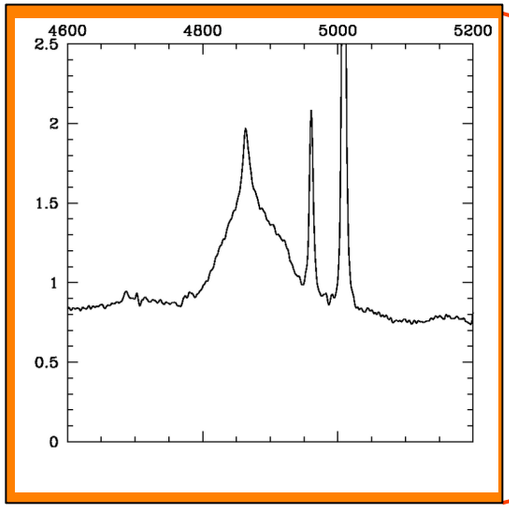

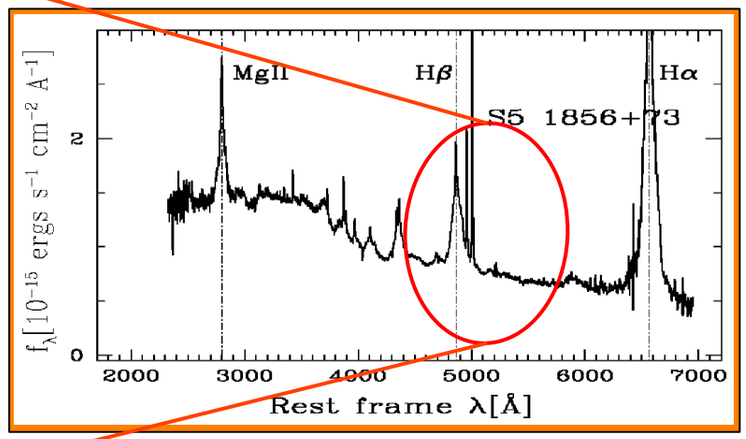

Hβ

NC

BC

VBC

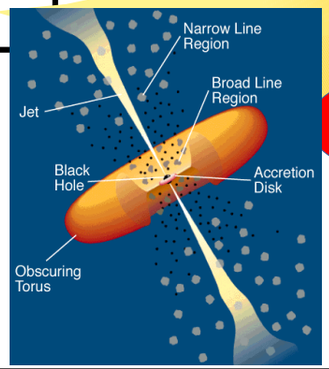

Intensity

Wavelength

FWHM

Skewness

Initial guess

Lower limit

Upper limit

Step size

Tolerance

Parameter nature

[OIII]λλ4959,5007

NC

SBC

HeIIλ4686

NC

BC/VBC

Method: Spectral fitting MgIIλ2798

Continuum

$$F_\lambda^{cont} = F_\lambda^{PL} + F_\lambda^{FeII} + F_\lambda^{BaC}.$$

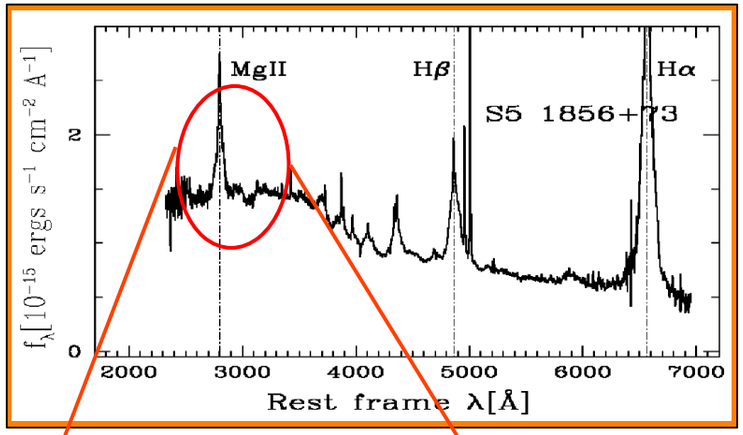

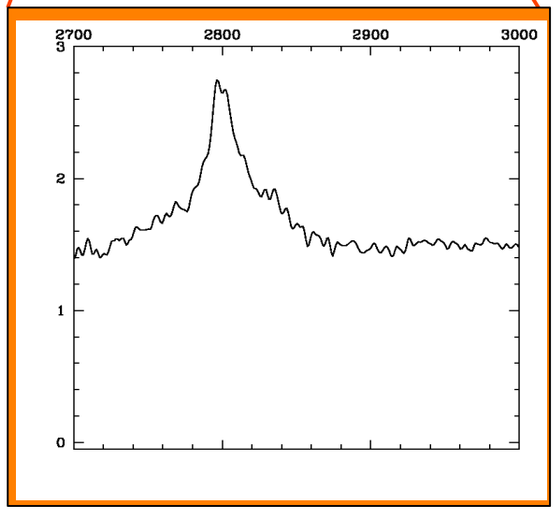

MgII

NC1, NC2

BC1, BC2

VBC

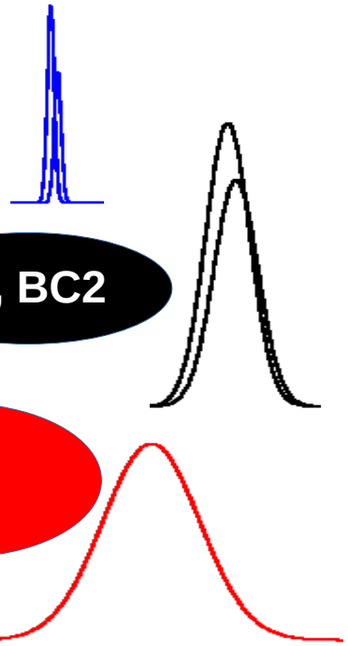

[Ne V]λλ3346,3424

NC

NC

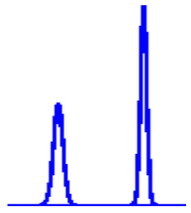

[OII]λ3728

NC

Method: Continuum fitting results

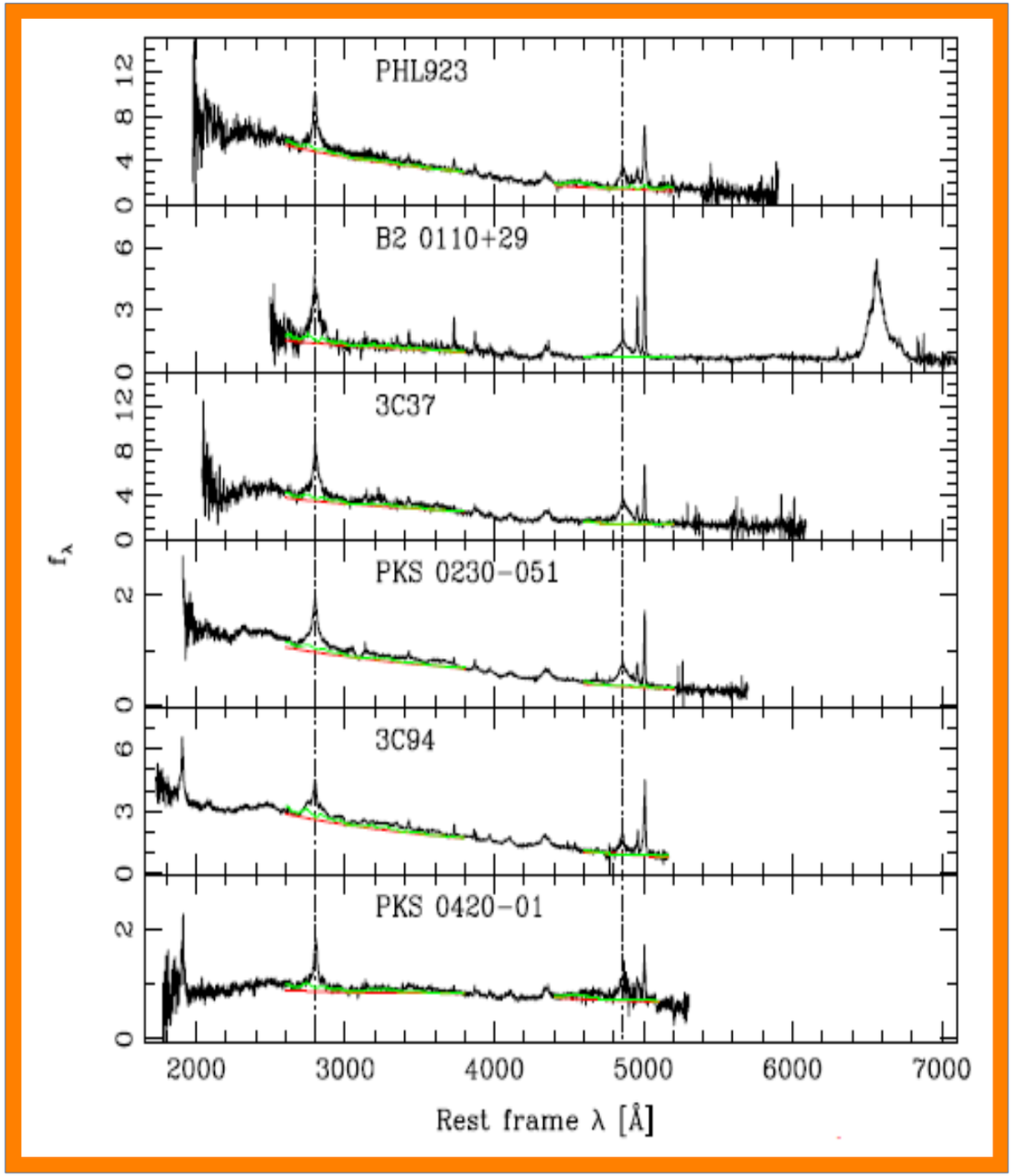

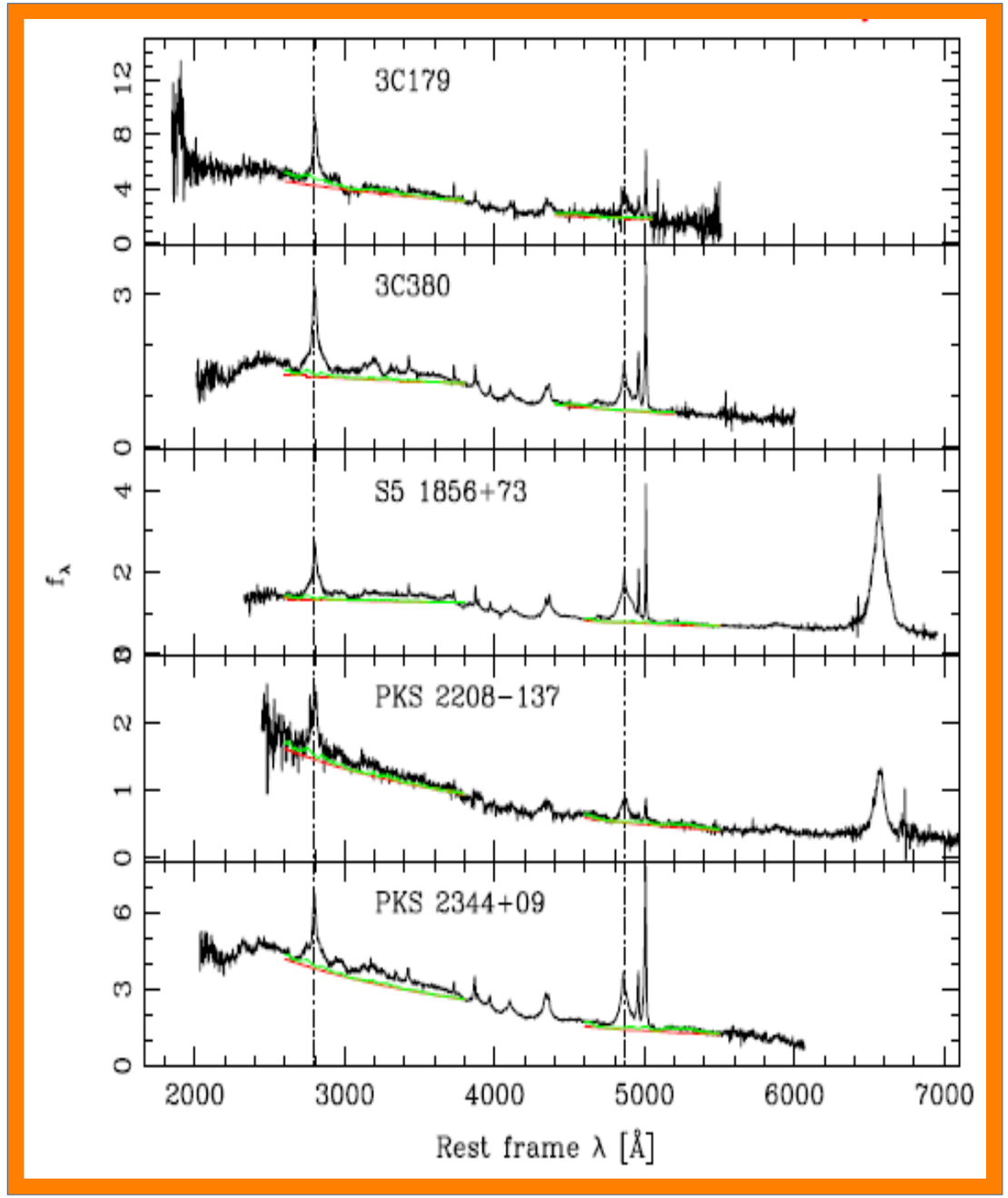

Fig **Rest-frame spectra and multi-component fitting continuum placement in the *Hβ* and *MgII* regions.**

Method: Emission lines fitting results

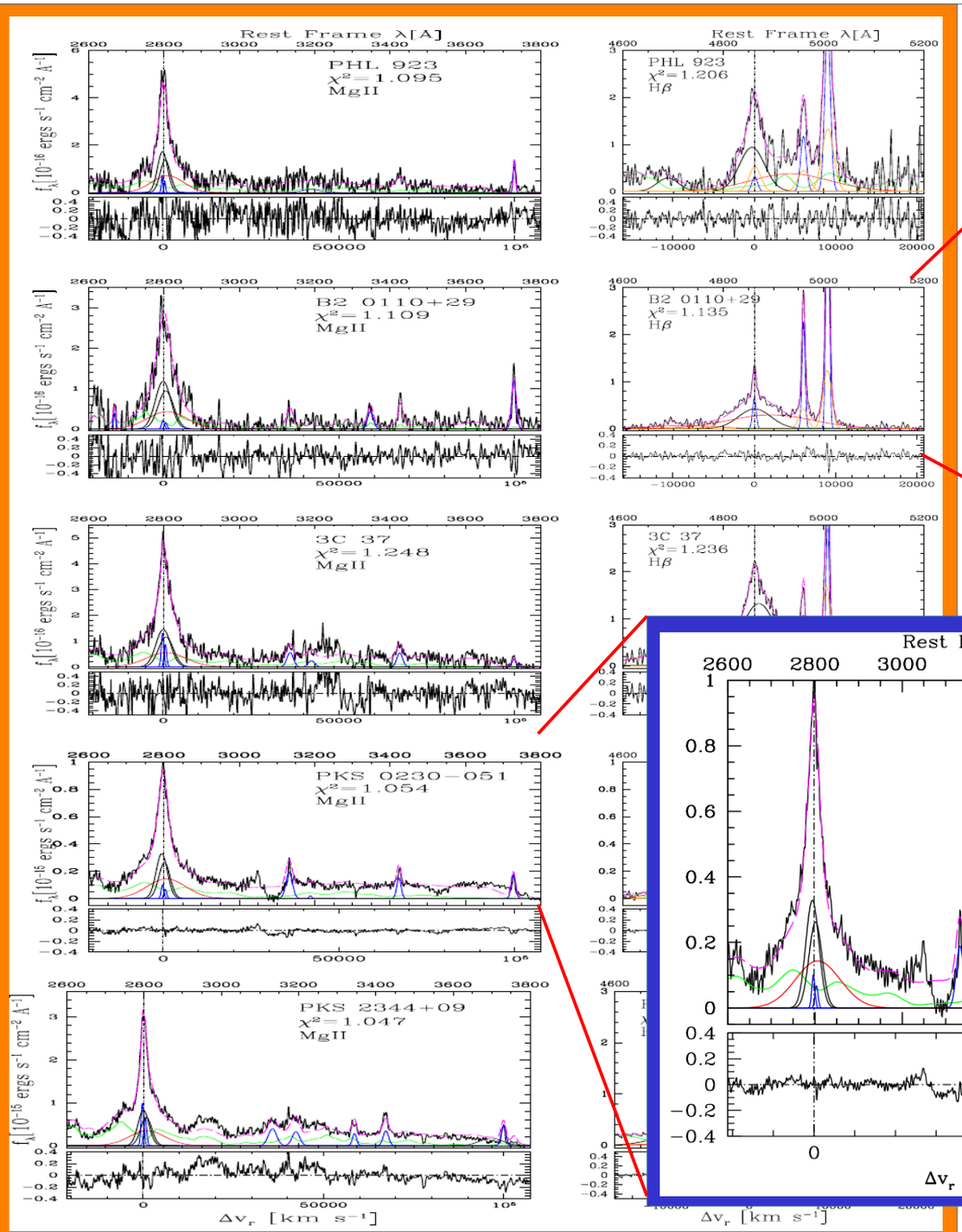

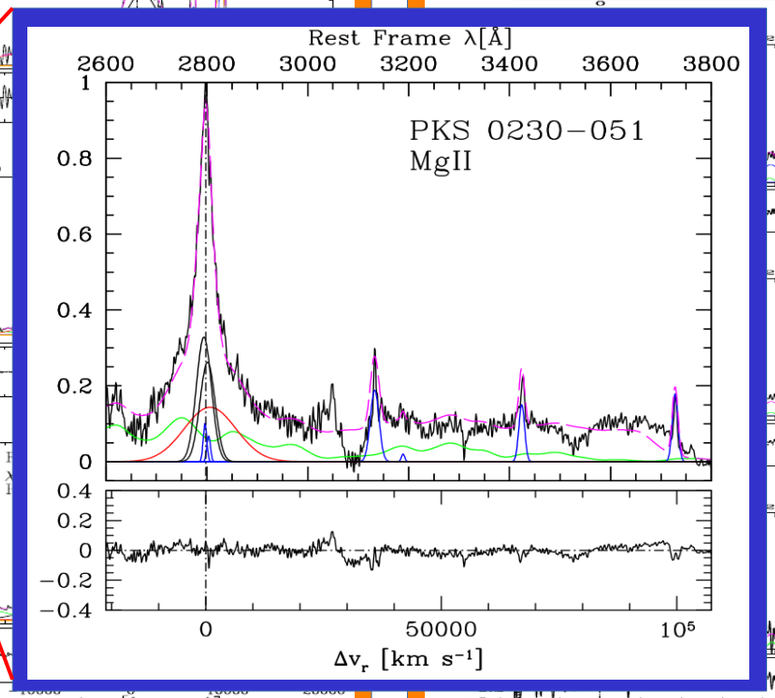

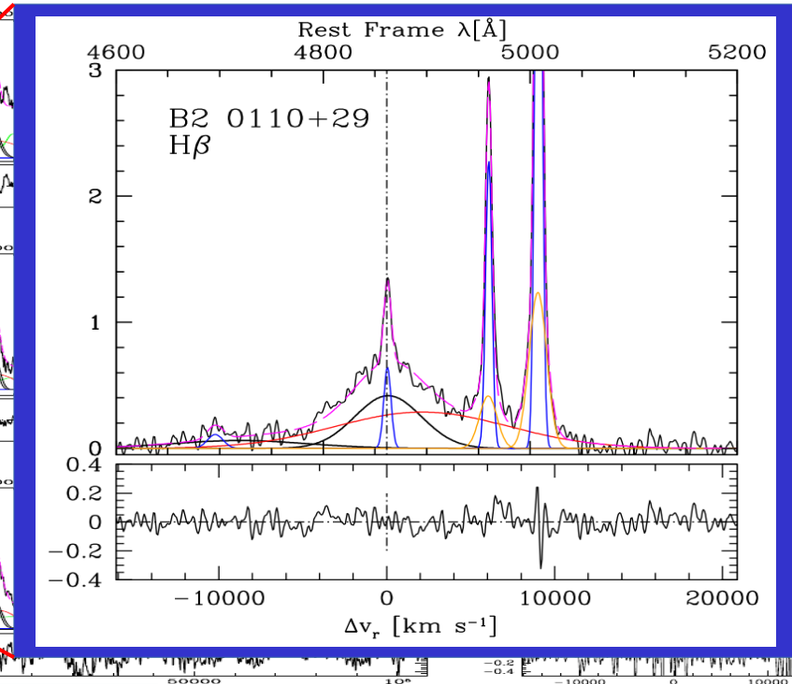

Method: 2. Full broad profile (FP) analysis

❖ **The FP represents the combined shape and intensity of different components.**

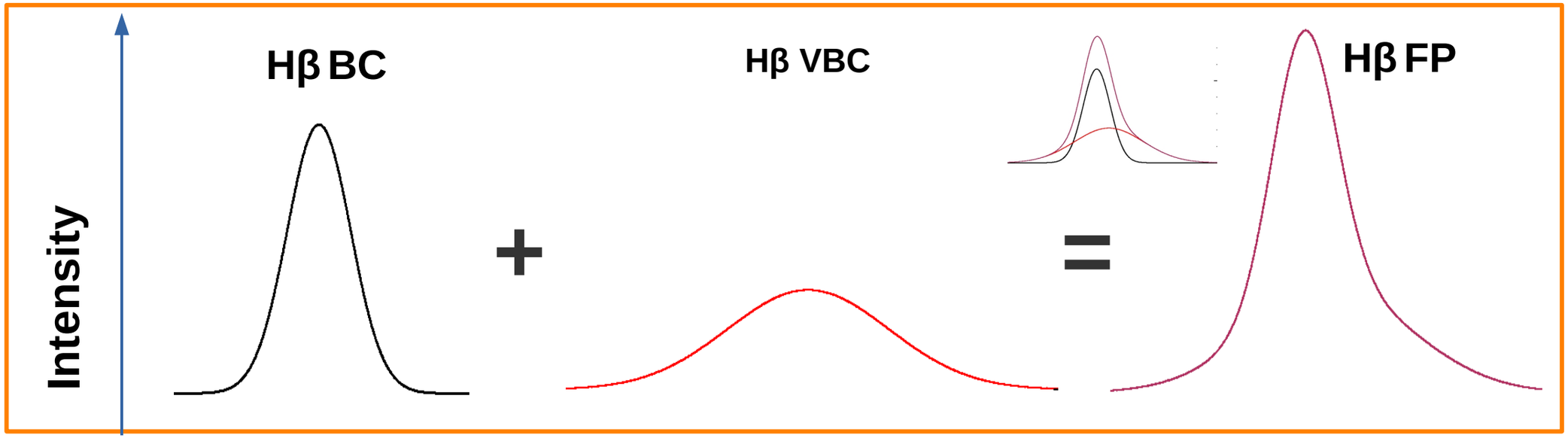

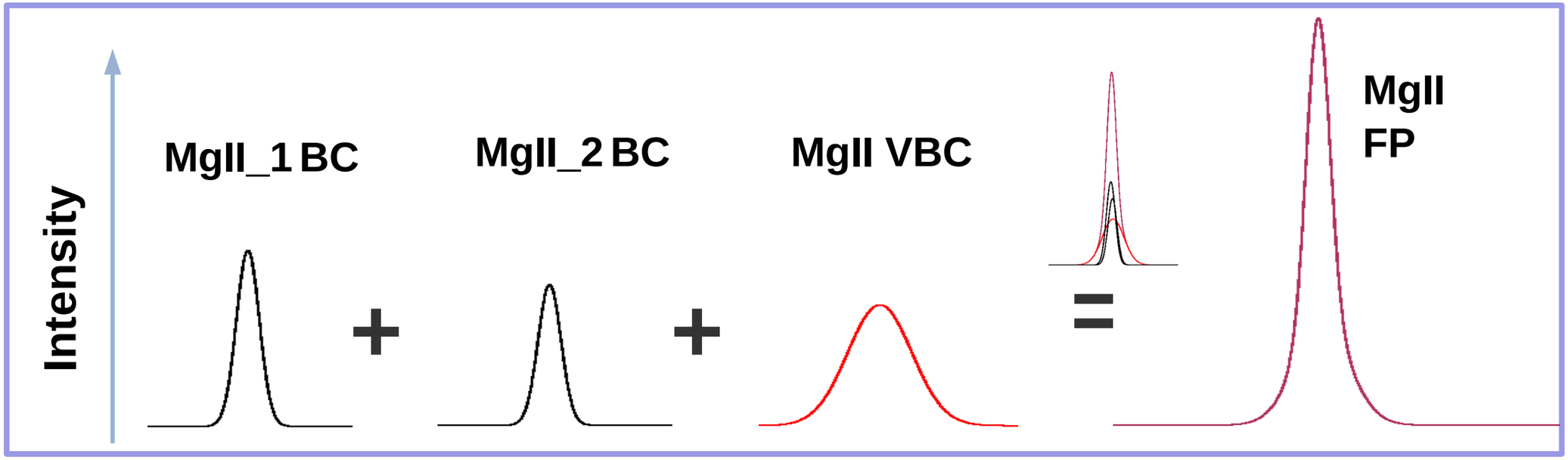

Method: Profile parameters

- **Profile parameters: to describe the shape and properties of the FP.**

- **The three important profile parameters are, centroid velocity, asymmetry index and Kurtosis index.**

Centroid velocity

$$c(x) = \frac{\upsilon_{r,R}(x) + \upsilon_{r,B}(x)}{2},$$

$\mathbf{x = {}^{i}/_{4}\ ,\ i = 1, 2 \text{ and } 3}$

Asymmetry Index

$$A.I = \frac{\upsilon_{r,R}(\frac{1}{4}) + \upsilon_{r,B}(\frac{1}{4}) - 2\upsilon_{r,peak}}{\upsilon_{r,R}(\frac{1}{4}) - \upsilon_{r,B}(\frac{1}{4})},$$

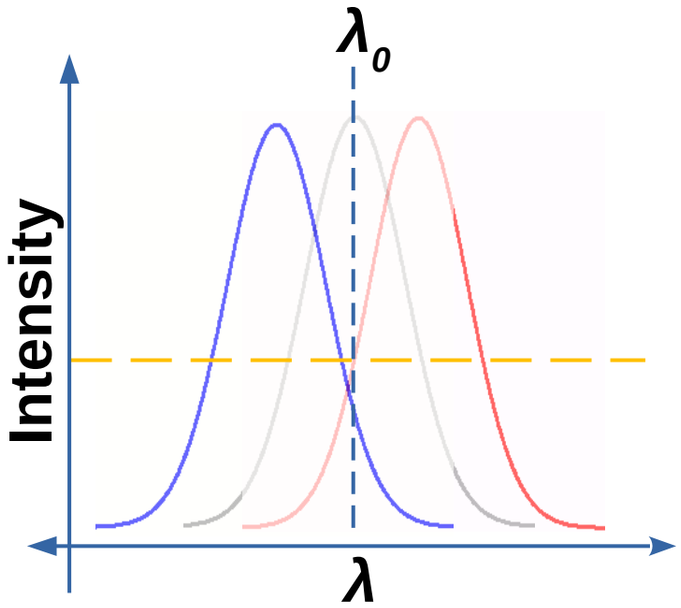

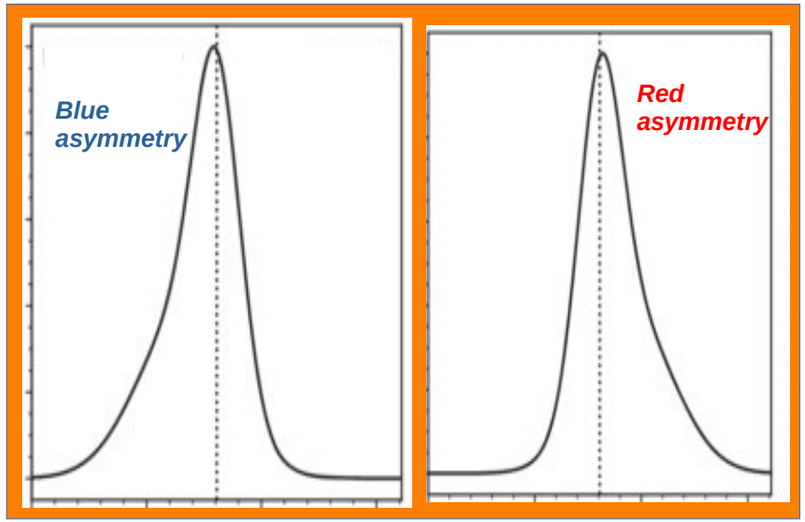

Credit: Pu Do et al. 2018

Results Part I

Optical and Near-UV Spectroscopic Properties of Low Redshift Jetted Quasars in the Main Sequence Context

Monthly Notices of the ROYAL ASTRONOMICAL SOCIETY

MNRAS **525**, 4474–4496 (2023) https://doi.org/10.1093/mnras/stad2467
Advance Access publication 2023 August 16

Optical and near-UV spectroscopic properties of low-redshift jetted quasars in the main sequence context

Shimeles Terefe Mengistue,[1,2,3★†] Ascensión Del Olmo,[4★] Paola Marziani,[5★] Mirjana Pović,[1,4,6] María Angeles Martínez-Carballo,[7] Jaime Perea[4] and Isabel Márquez[4]

Analysis results: Hβ fitting and Optical plane

- The optical plane formed from FWHM of Hβ and R_{FeII} in optical
- Median FWHM (Hβ) $\approx$ 5100 kms^{-1} and $R_{FeII} \approx$ 0.28
- A comparison sample taken from (Zamfir et.al., 2008, 2010)

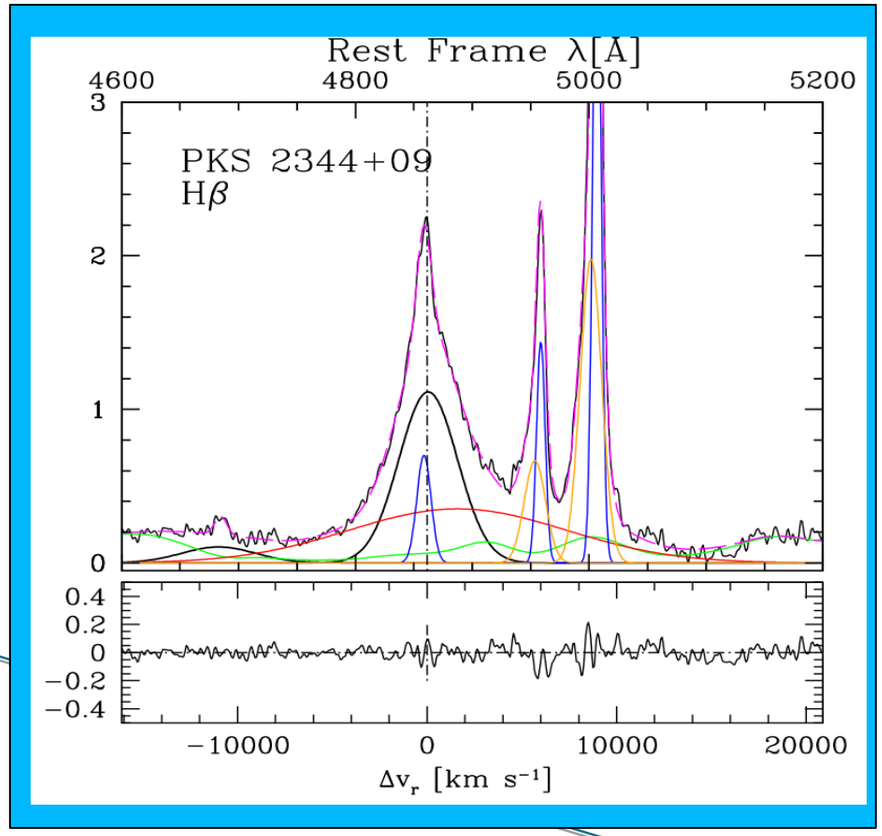

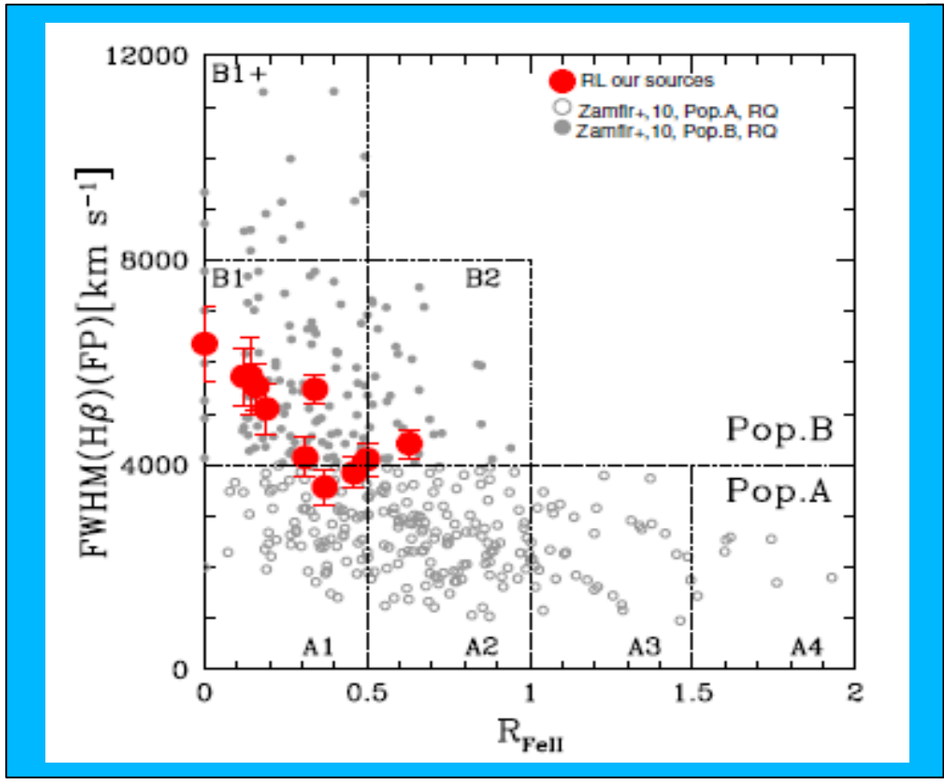

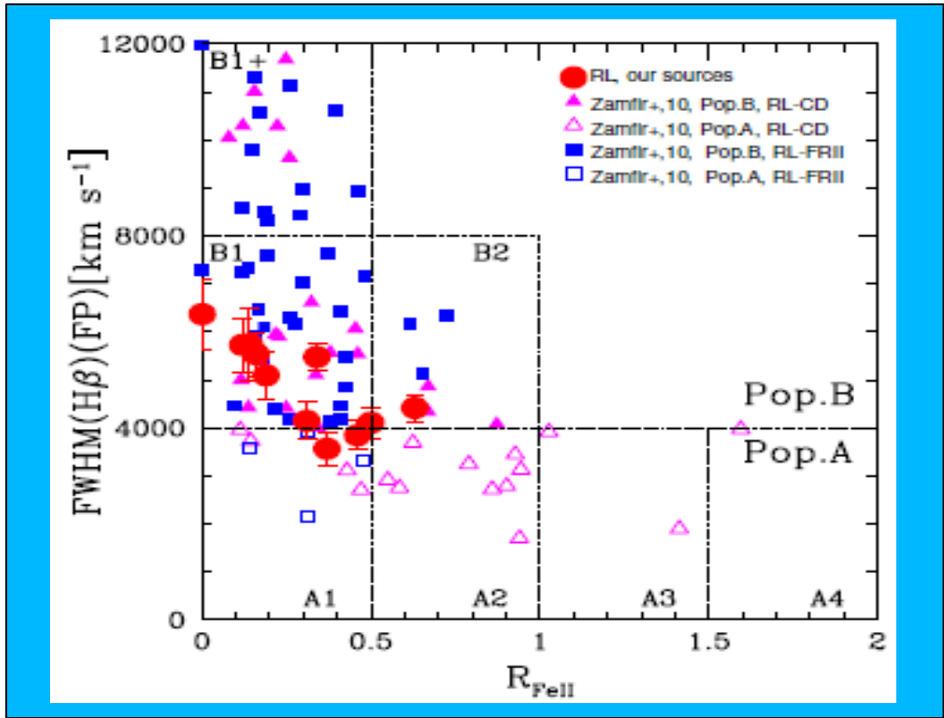

Analysis results: UV plane

- Formed from FWHM *MgII FP* and $R_{FeII} = I(FeII_{UV})/I(MgII_{FP})$.

- A comparison sample from Calderone et al. 2017 QSFit catalog.

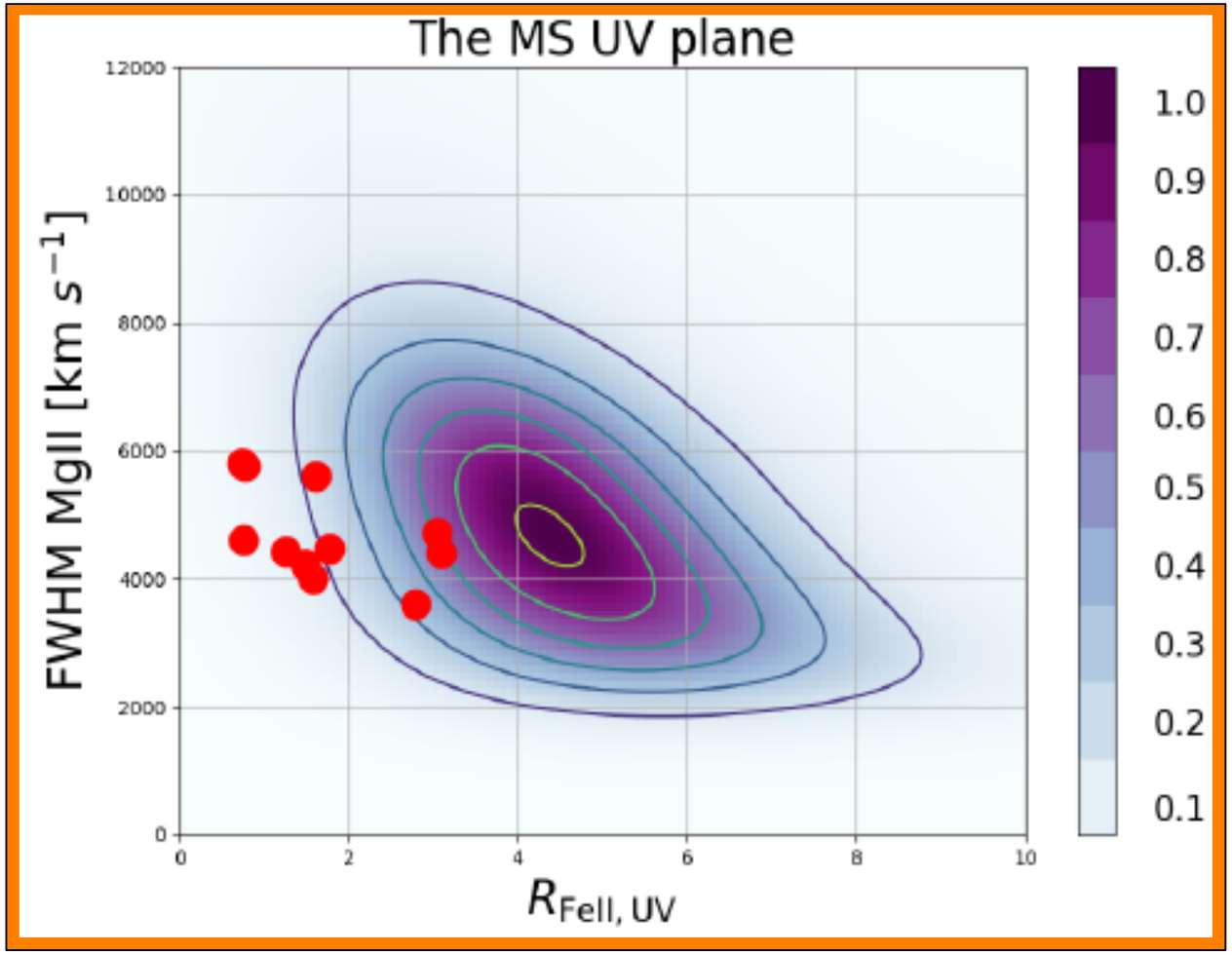

Fig. Placement of the 11 extremely jetted quasars on the UV plane defined by MgII FWHM Vs R_{FeIIUV} and a comparison sample after kernel smoothing

Comparison: Hβ and MgIIλ2800Å

- **Comparable strength *I(MgII)/I(Hβ) ~ 0.5 – 1.74***
- **FWHM Hβ(~5100 *km s^{-1}km s^{-1}*) > MgII(~ 4400 *km s^{-1}*) by 10% .**
- **Larger shift towards the red at line base (*c*(1/4)), less pronounced shift in MgII (~ *400 km s^{-1}*) than in Hβ (~ *1100 km s^{-1}*).**
- **Both profiles show redward asymmetry, MgII (0.02) is more symmetric than Hβ (0.4).**

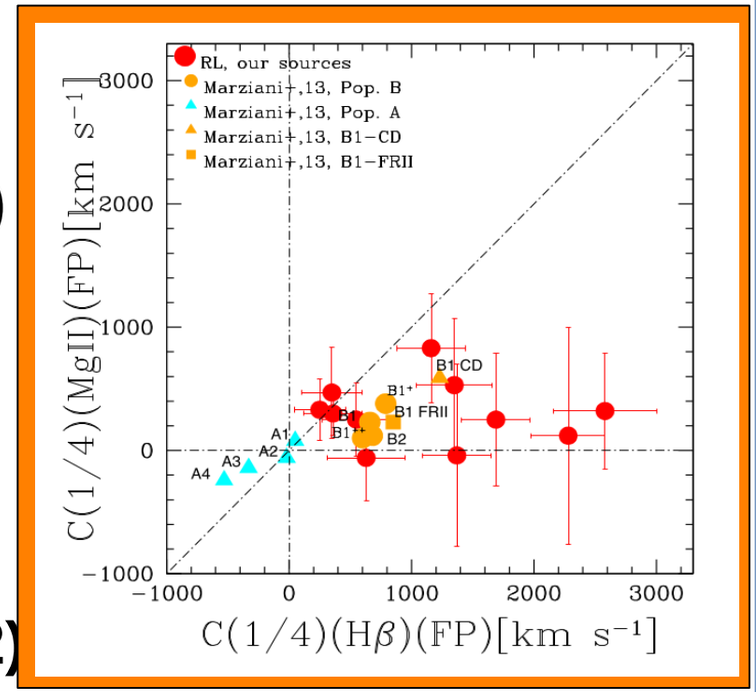

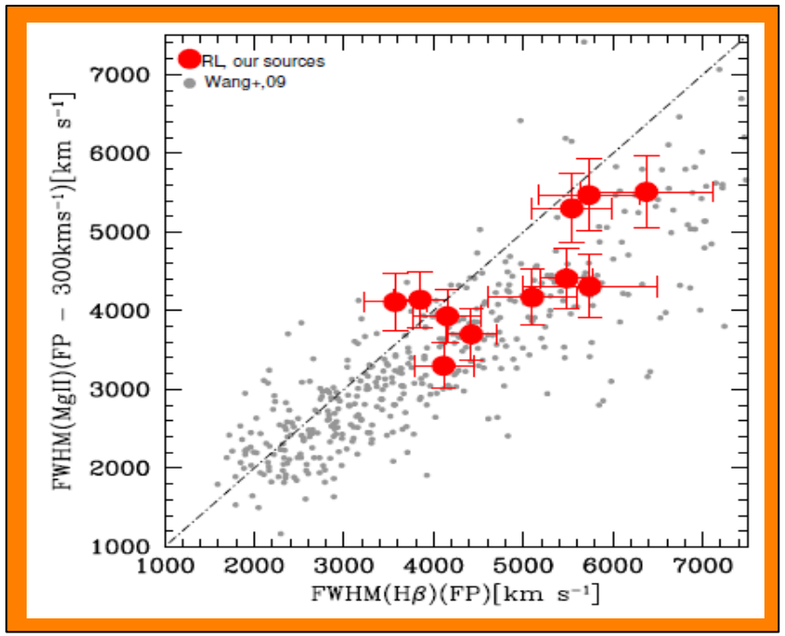

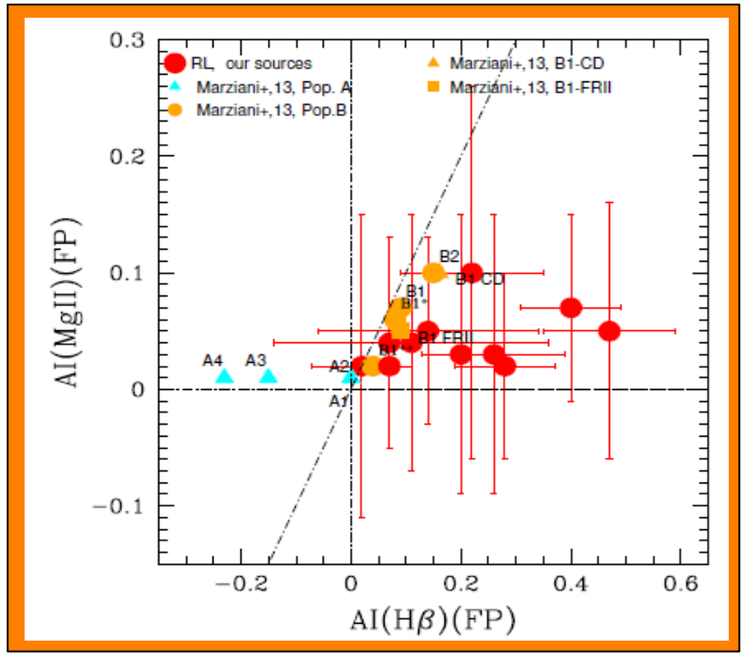

Fig. Comparison of the FWHM (left), centroid shift at the line base (right top) and asymmetry (right bottom) of the Hβ and MgII lines .

Black hole mass (M_{BH}) and Eddington ratio (λ_E)

- To estimate M_{BH} scaling relations using Vestergard & Peterson 2006 (Hβ) and Trankhtenbrot & Netzer 2012 (MgII).

$$LogM_{BH}(M_\odot) = Log\left\{\left[\frac{FWHM(H\beta)}{1000 kms^{-1}}\right]^2\left[\frac{\lambda L_\lambda(5100)}{10^{44} ergss^{-1}}\right]^{0.5}\right\} + (6.91 + 0.02)$$

- Continuum fluxes at 5100Å (3000Å) for Hβ and (MgII).
- $LogM_{BH}$ in the range from 8.5 $M_\odot$ to 9.5 $M_\odot$ using Hβ line.
- Relations from Trankhtenbrot & Netzer (2012) and Shen & Liu (2012) are good M_{BH} estimators while using MgII.
- $Log\lambda_E$ range from −1.45 to −0.55 (*Hβ*) and −1.40 to −0.78 (*MgII*)

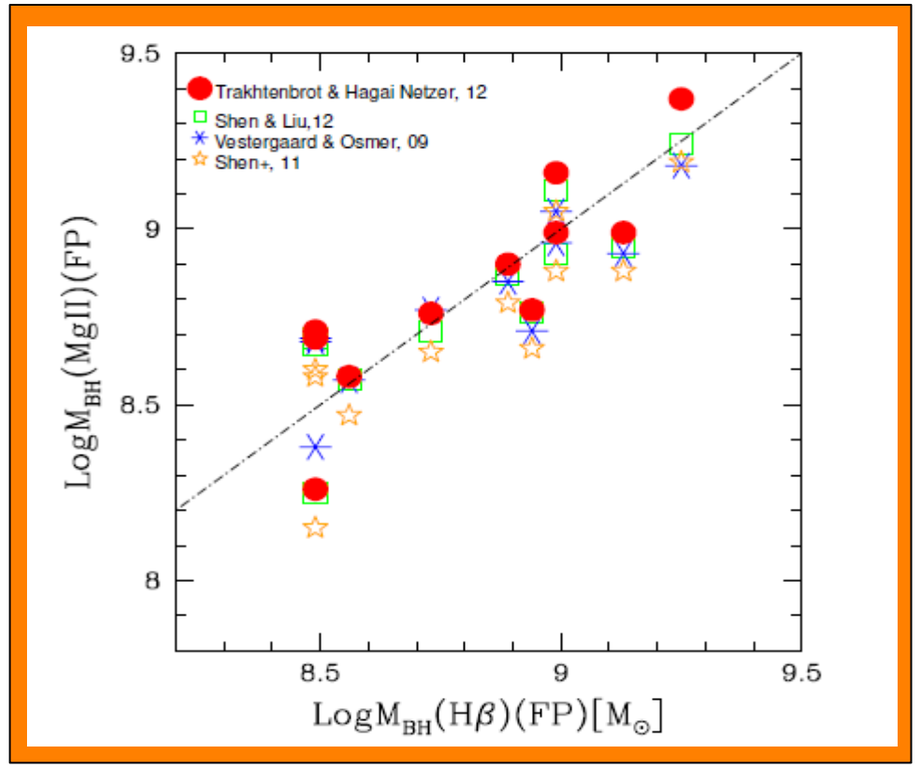

Fig. Comparison of M_{BH} estimates from different scaling relations.

Comparison: Physical and profile parameters

- A comparison is done based on their population and radio type
- For RLs, the velocity shift appears to be dependent on M_{BH} and λ_E:
  - Larger $c(1/4)$ occurs for the highest M_{BH} and lower λ_E

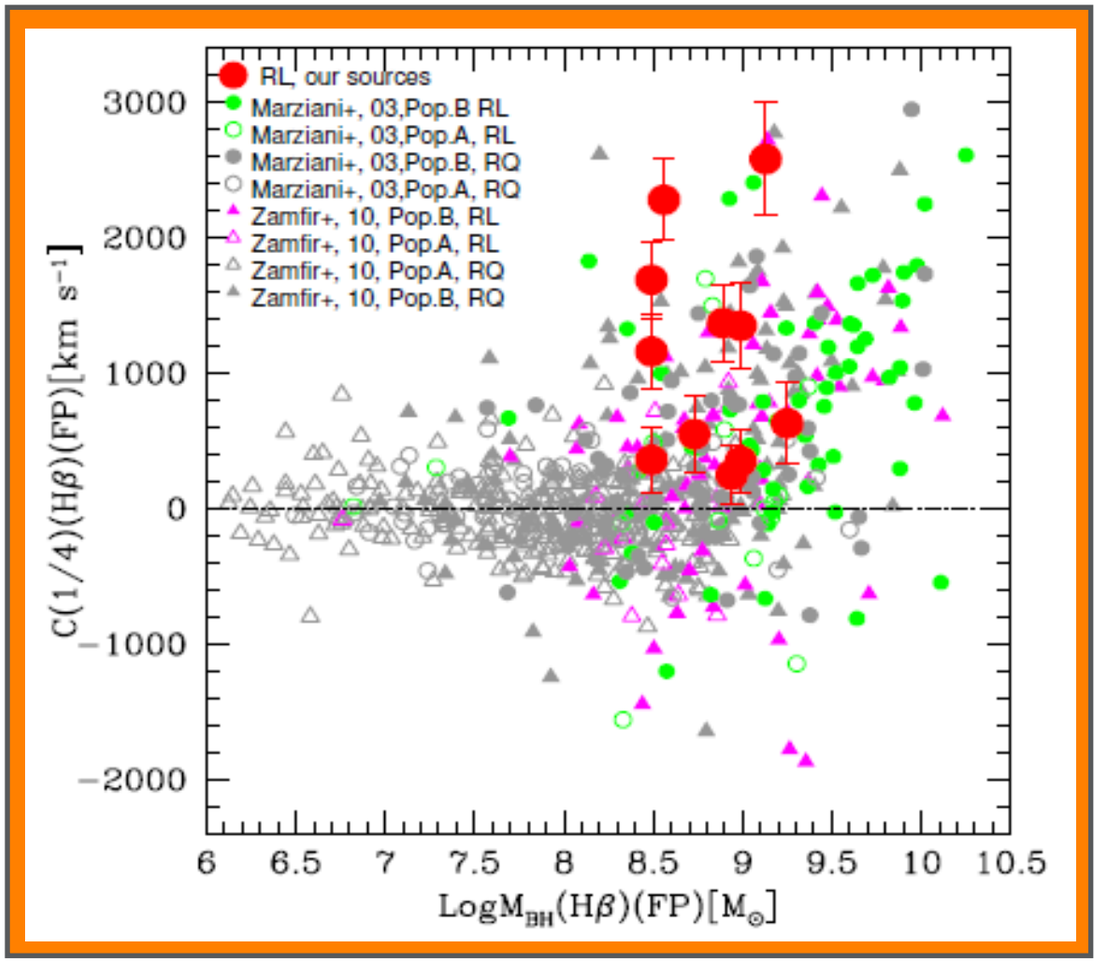

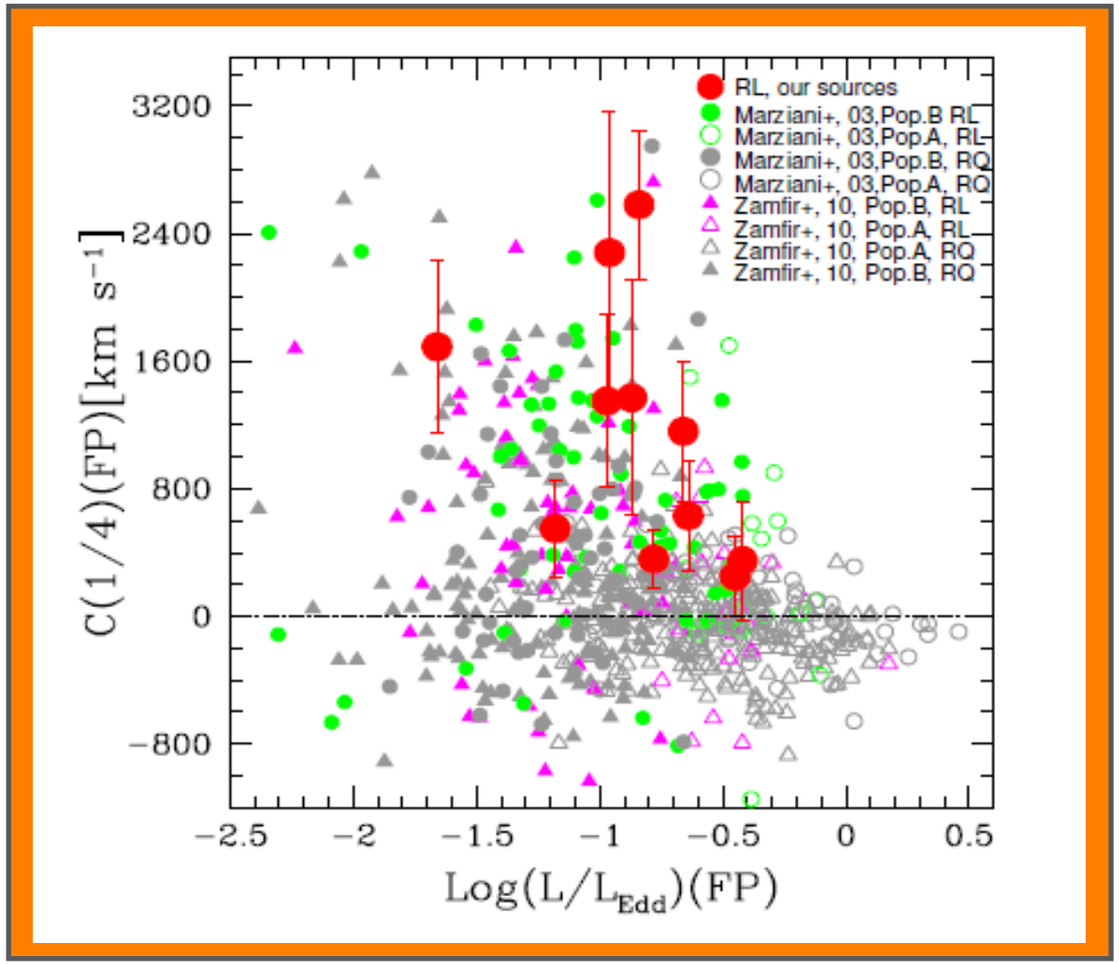

Fig. Dependence of centroid velocity shift on M_{BH} (left) and λ_E (right).

Comparison: RL and RQ quasars

- To see effect of R_k on the c(1/4), we considered RQ and RL within Pop. B only from Marziani et al. 2003, Zamfir et al. 2008 and this work:
  - 169 RQs, 145 RLs ($1.8 \leq \log R_K < 3$) and
  - 53 extreme RLs ($\log R_k > 3$)

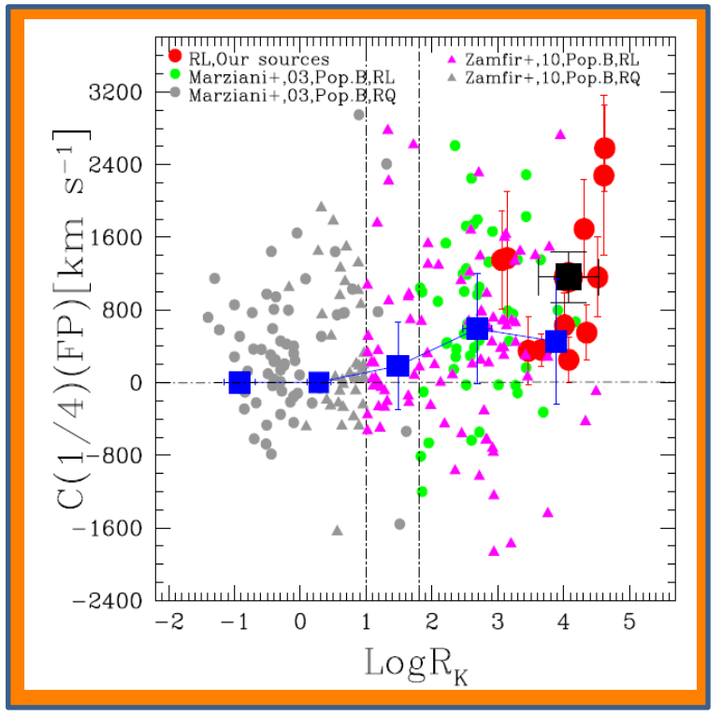

- There is a trend between the centroid velocity shift and R_k:
  - Pop. B RLs tend to have larger velocity shifts (740 km s^{-1}) than RQs (440 km s^{-1})
  - Larger for extreme RLs (1300 km s^{-1})

- Bootstrap replications of the RQ Pop. B considering only distributions of M_{BH} and λ_E consistent with the ones of RL Pop. B

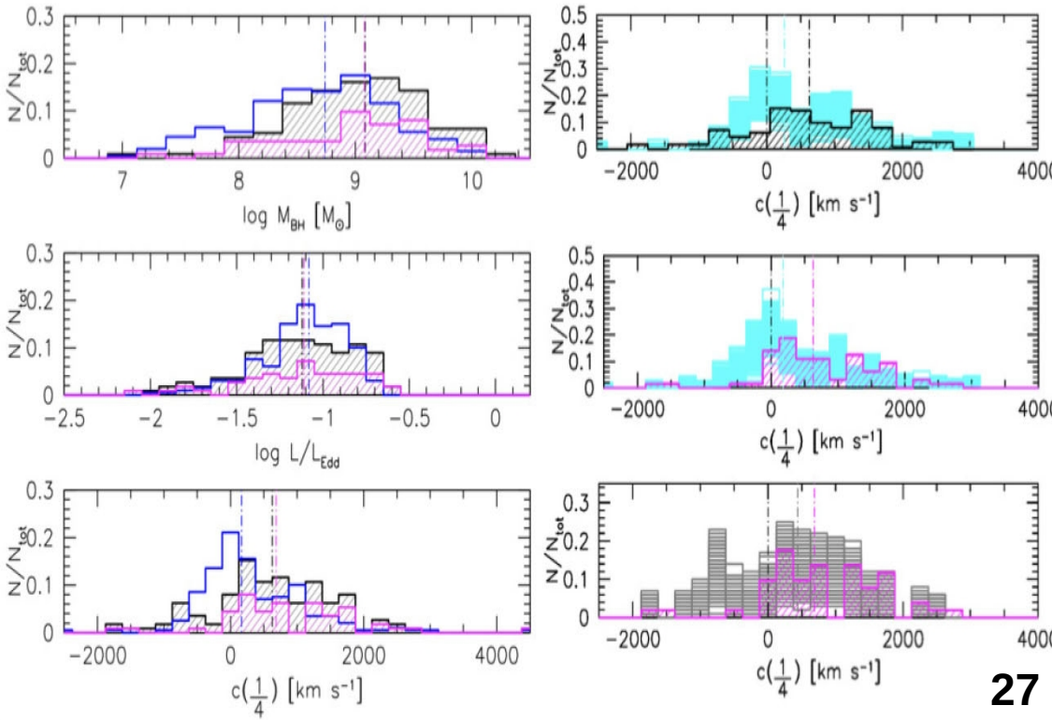

Fig. Relation between c(1 /4) of Hβ and R_k (top) and bootstrap analysis (bottom left) and bootstrap replication results (bottom right).

Summary

- **Possible to quantifying the broad emission line difference between RL and RQ quasars by implementing the 4DE1 parameter space**
  (Provides spectroscopic contextualization for all the type-1 AGN).

- **RL quasars exhibit a larger Hβ FWHM weaker FeII emission, and distinct characteristics in the optical and UV main sequence planes.**
  (A restricted domain occupation confirmed)

- **Only the most powerful RL quasars display stronger shift, redward asymmetries, larger M_{BH} and low L_{Bol}/L_{Edd} with respect to the RQ.**
  (Improves understanding of the physical processes taking place around the SMBH)
- **It also provides a piece of evidence to assert the potential dichotomy between RL and RQ quasars, (solve the debated problems associated with bimodality or a real physical dichotomy between them.)**


THANK YOU